Optimization Strategy for Shape Control of Aircraft Composite Panels Based on Flexible Tooling

WANG Qi[1], *ZHANG Pin*[1], *YU Jixuan*[1], *MENG Xiangmin*[1], *WANG Kuikui*[1], *ZHAO Cong*[2*], *ZHANG Xuezhuang*[2], *LI Xinxin*[2]

1. Aeronautical Science and Technology Key Laboratory of High Performance Electro-Magnetic Windows, AVIC Research Institute for Special Structures of Aeronautical Composites, Jinan 250023, P. R. China; 2. College of Mechanical and Electrical Engineering, Nanjing University of Aeronautics and Astronautics, Nanjing 210016, P. R. China

(Received 8 May 2025; revised 22 September 2025; accepted 30 September 2025)

Abstract: Composite materials have been widely applied to aircraft structures due to their significant mechanical performance and lightweight. However, the shape difference, which induced by curing deformation, between the actual and theoretical composite panels leads to poor assembly accuracy. This paper proposes a shape control method with flexible tooling based on the finite element analysis and the adaptive genetic algorithm. The optimized displacement of every distributed shape adjusting end can be calculated to meet the requirements for shape conformity and structural healthy of the composite panel. The feasibility of the method has been verified via the shape optimization of aircraft wing-body fairing composite panel. Experimental results indicate that the shape conformity (within 0.3 mm) increases from 66.46% to 86.36% with the proposed optimized method. Moreover, the accuracy and efficiency for the composite panel assembly have been significantly improved. This study provides a new efficient and accuracy approach for the shape adjustment of composite panels during the assembly process.

Key words: composite materials; aircraft assembly; shape control; optimization strategy; genetic algorithm

CLC number: TB330.1 **Document code:** A **Article ID:** 1005-1120(2026)02-0301-16

0 Introduction

Composite parts are increasingly widely used in civil aircraft due to their outstanding mechanical performance and weight saving effects[1-5]. To guarantee the aerodynamic profile, the shape accuracy of composite panel should be well controlled. However, the deformation of composite panel introduced in the curing process often leads to difference between actual and theoretical shapes of the composite panel[6]. In such a condition, the shape of the composite panel should be modified to meet the requirements of assembly accuracy. With growing scale of composite panel used in aircraft, the time of whole shape control process increases dramatically. Meanwhile, the anisotropic performance of composite makes precise adjustment of composite panel more difficult. Moreover, inappropriate shape optimization method may introduce large stress in composite panel, which may result in the appearance of damage. Therefore, efficiency methods for the shape control of composite panel, considering the shape accuracy and mechanical performance, require addressing.

In recent years, the substitution of traditional rigid tooling with intelligent and flexible assembly systems has emerged as one of the development directions for enhancing assembly quality, which can

*Corresponding author, E-mail address: zhaocong_ccme@nuaa.edu.cn.

How to cite this article: WANG Qi, ZHANG Pin, YU Jixuan, et al. Optimization strategy for shape control of aircraft composite panels based on flexible tooling[J]. Transactions of Nanjing University of Aeronautics and Astronautics, 2026, 43(2): 301-316.

http://dx.doi.org/10.16356/j.1005-1120.2026.02.010

precisely control the displacement or load applied on the composite panel for the shape adjustment[7-8]. Ramirez et al.[9] developed a flexible supporting tooling system with modular clamping unit, which could achieve the positioning and shape adjustment for different composite panels. Yang et al.[10] proposed a shape control method for composite fuselage panel assembly, based on multi-robotic tooling system. The maximum shape deviation can be controlled less than 0.6 mm. Liu et al.[11-12] developed an effective method to adjust the shape of composite panel with distributed modular adjusting units. Wu et al.[13] proposed a force application strategy to reduce the gap between the skin and the framework of aircraft. The average scale of gap was 0.15 mm. Furthermore, Zhang et al.[14-16] established a finite element model to optimize the size and layout of the compression force for composite panel shape adjustment, considering the interlamination behavior of composites. Jiang[17] proposed a method to achieve good accuracy of composite panels and less induced stress during the assembly process. Based on the tooling mentioned in Ref.[16], the maximum stress of the panel after optimization was only 51.7% of that before optimization. Zhang[18] proposed a shape control technology of composite panels based on actual measurement data. However, the scale of composite panel applied to aircraft is getting larger and larger. Accurate and efficiency method for the shape control of the large scaled composite panel should be further studied.

In this paper, a shape control method for the composite panel with flexible tooling is proposed, based on the finite element analysis and the adaptive genetic algorithm, which can provide the shape optimization method automatically for different sized composite panels during their assembly process. The optimized displacement of every single displacement applying unit can be calculated to meet the requirements for shape conformity and structural healthy of the composite panel. The feasibility of the method has been verified via the shape optimization of the aircraft wing-body fairing composite panel. The accuracy and efficiency for the composite panel assembly can been significantly improved. This study provides a new efficient and accuracy approach for the shape adjustment of composite panels during the assembly process. Moreover, the results of this paper can also provide a reference for the design of flexible tooling for the shape adjustment of composite panels, which can achieve the shape optimization automatically.

1 Shape Optimization Process of Composite Panels

As shown in Fig.1, the process of shape optimization for the composite panel proposed in this paper includes the establishment of the optimization model, the initialization of the finite element model, the parameter setting of the optimization algorithm, the expression of variables in the finite element, and the solution of the optimization model. The problem to be solved can be described as the optimization problem of the composite panel adjustment with the two goals. On one hand, the deviation between the actual shape and the theoretical shape of the panel should be minimized to improve the shape accuracy of the panel. On the other hand, the damage in the composite panel should be avoided to achieve good mechanical performance. Based on the numerical analysis method and the proposed ntelligent optimization algorithm, the above optimization problem can be solved.

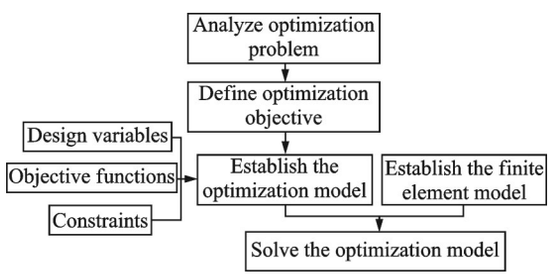

Fig.1 Process of shape optimization for composite panel

2 Establishment of Optimization Model

Establishment of the optimization model is critical to solving optimization problems[19]. Specifically, once the optimization objectives are clarified, three core elements of the optimization problem should be defined, including design variables, objective functions, and constraint conditions.

2.1 Design variables

In the flexible tooling involved in this paper, the shape of the composite panel is adjusted via the distributed shape-adjusting ends, which can apply concentrated force or local displacement on the composite panel to change the shape of the composite panel. To simplify the control process, local displacement is chosen as the output of the distributed shape-adjusting ends. In such way, the layout and the magnitude of concentrated force or local displacement used by distributed shape-adjusting end should can be considered as design variables.

In order to express the layout and magnitude of the distributed shape-adjusting ends more clearly, $h_i(i=1,2,\cdots,n)$ and $l_i(i=1,2,\cdots,n)$ are set as the location and the magnitude of the displacement, respectively, used by the ith distributed shape-adjusting end. Then, the layout and the magnitude of displacement, used by distributed shape-adjusting ends, can be expressed as $H=\{h_1,h_2,\cdots,h_n\}$ and $L=\{l_1,l_2,\cdots,l_n\}$, respectively, where n is the number of distributed shape-adjusting ends. Thus, the design variables can be expressed as

$$X=[H,L] \tag{1}$$

Taking the practical condition into account, the value range of design variables can be described as follows:

First, the number of distributed shape-adjusting ends n, involved in the shape adjustment, should be less than the total number of distributed shape-adjusting ends N in the flexible tooling.

Second, the magnitude of displacement used by the distributed shape-adjusting end should be larger than $-L_{\max}$, but less than $L_{\max}$, which is determined by the distributed shape-adjusting end.

2.2 Objective function

The main objective of this paper is to find an optimization method for the shape control of composite panels based on flexible tooling, which can make the deviation between the actual and the theoretical shapes of the panels as small as possible. Meanwhile, damage in the composite panel should be avoided during the shape adjustment process. Therefore, the shape accuracy is set as the objective function of the optimization model. While, the constraints can be considered as that there is no damage in the composite panel.

In order to qualify the shape accuracy of the panel, the profile compliance rate of the composite panel $R(X)$ is defined, which is a statistical function calculated by the deviation of corresponding monitoring points between the theoretical and the actual shapes in normal direction. Detailed calculation of the profile compliance rate can be described as follows.

As shown in Fig.2, taking the monitoring point i as an example, λ_i represents the spatial coordinate of the displacement monitoring point i on the actual shape. φ_i denotes the projection point's spatial coordinate of monitoring point i on the theoretical shape, along the normal direction of actual shape at monitoring point i. Thus, the shape deviation ω_i between actual and the theoretical shapes in monitoring point i can be calculated by

$$\omega_i=\lambda_i-\varphi_i \tag{2}$$

During the shape adjustment process, the displacement in $\Delta\omega_i$ in normal direction of the actual shape at monitoring point i can be introduced via dis-

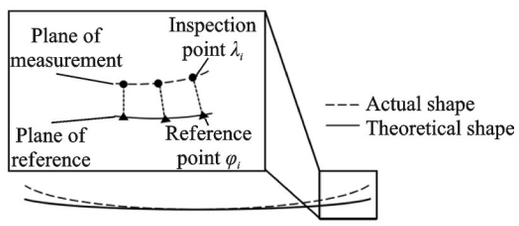

Fig.2 Schematic diagram of shape deviation calculation

tributed shape-adjusting ends. The final shape deviation of the panel after adjustment can be described as

$$\omega_i' = \omega_i + \Delta\omega_i \tag{3}$$

The allowable value of the shape deviation of the panel is $\Delta\omega$, which can be determined via the assembly process specifications. According to the relationship between $|\omega_i'|$ and $\Delta\omega$, the status of the profile compliance of the composite panel at monitoring point i, $G_i(X)$ can be expressed as

$$G_i(X) = \begin{cases} 1 & |\omega_i'| \leqslant \Delta\omega \\ 0 & |\omega_i'| \geqslant \Delta\omega \end{cases} \tag{4}$$

When the status meets the requirement on the profile compliance of the composite panel at monitoring point i, $G_i(X)=1$. Otherwise, $G_i(X)$ is conversely recorded as 0.

Thus, the profile compliance rate of the composite panel $R(X)$ can be determined according to

$$R(X) = \frac{1}{t}\sum_{i=1}^{t} G_i(X) \tag{5}$$

where t is the total number of monitoring points.

The higher the value of $R(X)$ is, the less shape deviation between the actual and theoretical shape of the panel can be achieved.

2.3 Constraints

As mentioned in Section 2.2, the constraint in the process of shape control for composite panels is that no damage occurs within the composite panel.

To predict the damage occurrence and its propagation in composites, many failure criteria have been proposed for different conditions[20], such as maximum strain or maximum stress criterion, Tsai-Hill criterion, Tsai-Wu criterion and Hashin criterion. Even though the progressive damage and fatigue effects were ignored in 3D Hashin criterion, the occurrence of composite damage under out-of-plane stress can be predicted rapidly and accurately[21-23]. Therefore, 3D Hashin criterion was chosen to predict the damage initiation during the shape adjustment of the composite panel to reduce the shape optimization process cost and ensure relatively precision, which could be expressed as Eq.(6)[24].

$$\begin{cases} D_1(X) = \left(\dfrac{\sigma_{11}}{X_{1T}}\right)^2 + \left(\dfrac{\sigma_{12}}{X_{12}}\right)^2 + \left(\dfrac{\sigma_{13}}{X_{13}}\right)^2 & \sigma_{11} \geqslant 0 \\ D_2(X) = \left(\dfrac{\sigma_{11}}{X_{1C}}\right)^2 & \sigma_{11} < 0 \\ D_3(X) = \left(\dfrac{\sigma_{22}}{X_{2T}}\right)^2 + \left(\dfrac{\sigma_{12}}{X_{12}}\right)^2 + \left(\dfrac{\sigma_{23}}{X_{23}}\right)^2 & \sigma_{22} \geqslant 0 \\ D_4(X) = \left(\dfrac{\sigma_{22}}{X_{2C}}\right)^2 + \left(\dfrac{\sigma_{12}}{X_{12}}\right)^2 + \left(\dfrac{\sigma_{23}}{X_{23}}\right)^2 & \sigma_{22} < 0 \\ D_5(X) = \left(\dfrac{\sigma_{33}}{X_{3T}}\right)^2 + \left(\dfrac{\sigma_{12}}{X_{12}}\right)^2 + \left(\dfrac{\sigma_{23}}{X_{23}}\right)^2 & \sigma_{33} \geqslant 0 \\ D_6(X) = \left(\dfrac{\sigma_{33}}{X_{3C}}\right)^2 + \left(\dfrac{\sigma_{13}}{X_{13}}\right)^2 + \left(\dfrac{\sigma_{23}}{X_{23}}\right)^2 & \sigma_{33} < 0 \end{cases} \tag{6}$$

where $D_1(X)$—$D_6(X)$ represent the failure status of composites under the fiber tensile mode, the fiber compressive mode, the matrix tensile mode, the matrix compressive mode, the tensile delamination mode, and the compressive delamination damage mode. When any one of these values is greater than or equal to 1, it indicates that the corresponding type of damage has occurred in the composite material[23]; σ_{mn} $(m, n=1,2,3)$ is the stress introduced in the composite panel in different directions during the shape adjustment process, which can be obtained by finite element analysis (FEA).

During the composite panel shape optimization process, to prevent material damage, the values of $D_1(X)$—$D_6(X)$ should be less than 1. The constraints can be described as

$$D(X) = \max\{D_1(X), D_2(X), \cdots, D_6(X)\} \tag{7}$$

where $D(X)<1$.

2.4 Mathematical expression of optimization model

In summary, the optimization model of the shape optimization process of composite panels can be described as

$$\begin{cases} \max\{R(X)\} \\ R(X) = \dfrac{1}{t}\sum_{i=1}^{t} G_i(X) \\ n \leqslant N, -L_{\max} \leqslant l_i \leqslant L_{\max} \\ D(X) < 1 \end{cases} \tag{8}$$

where $R(X)$ is the objective function of the optimization model; $X=[H, L]$ the design variable, in-

cluding the layout of distributed shape-adjusting end involved in the optimization process and the magnitude of displacement applied by distributed shape-adjusting end; n and N are the number of distributed shape-adjusting end involved in the process and the total number of distributed shape-adjusting end in flexible tooling, respectively; L_{max} is the maximum displacement applied via shape-adjusting end; and $D(X)$ the failure status of the composite panel.

3 Solution of Optimization Model

3.1 Selection of solution method

Once the optimization model is established, the appropriate numerical analysis method and intelligent optimization algorithm should be determined to solve the optimization problem effectively.

Many intelligent methods have been proposed to solve different kinds of optimization problems[25-26], including simulated annealing (SA), genetic algorithm (GA), and particle swarm optimization (PSO). Compared with other intelligent optimization algorithms, GA has shown better performance on the versatility, global search ability, and designability. Furthermore, GA is more suitable than other algorithms to solve optimization problems with poor continuity of objective function values[27-30]. Considering the nonlinear relationship between the design variables and the objective function in the shape adjustment process of the composite panel, GA is employed to solve the optimization problem proposed in this paper.

The GA process involved in this paper is shown in Fig.3.

As mentioned before, owing to its high accuracy in solving nonlinear analysis problems, FEA is selected to predict the stress and damage initiation in the composite panel during the shape adjustment process.

Since ABAQUS provides subroutine interfaces for Fortran and plugin interfaces for Python, subroutines have been developed for ABAQUS to complete pre-processing and post processing, enabling automatic iterative calculations in ABAQUS. With

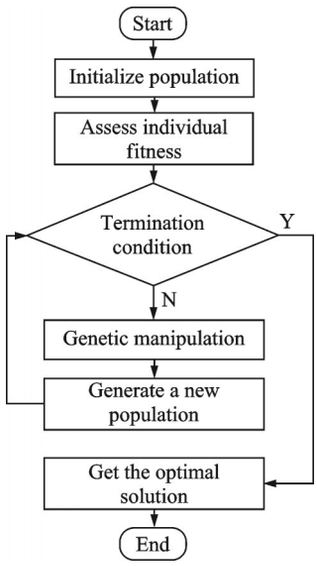

Fig.3 Flow chart of GA

the optimization iteration function of GA, the optimal solution is finally obtained. The solution strategy of shape optimization problem is shown in Fig.4.

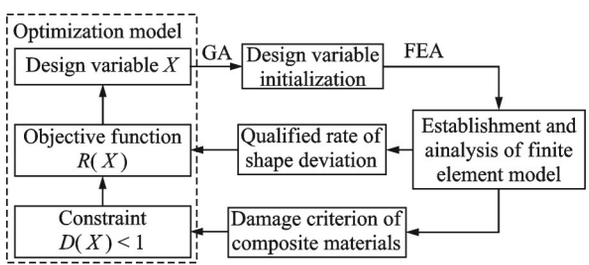

Fig.4 Optimization model solving strategy

3.2 Gene representation and encoding of design variables

In GAs, each individual consists of several genes, and multiple individuals form a population. As the basic unit for genetic operator operations, genes require design variables to be represented as gene-form individuals when solving optimization models. The design variables of the optimization model in this paper include layout component H and magnitude component L, which are represented by the layout and displacement of distributed shape-adjusting ends involved in the shape optimization process. n is the number of distributed shape-adjusting ends. Therefore, an individual in GA contains $2n$ genes. To represent solutions in a computer-processable form and provide a unified solution space for optimization, the above parameters should be encod-

ed. Common encoding methods include binary encoding, real-number encoding, matrix encoding[31]. Considering its great performance on adaptability, ease of implementing crossover and mutation operations, binary encoding is adopted in this paper.

3.3 Generation of design variables

(1) Selection operator

In each iteration of GA, the selection operator is used to screen individuals from the current population as the parent of the next generation. The selection process is based on probability, and the probability of selecting an individual is directly proportional to its fitness, and the higher the fitness, the greater the probability that the individual will be selected. In this paper, a roulette selection method is adopted, in which the selection probability of each individual is directly related to its fitness value. The selection process incorporates an elite strategy, which retains the fittest individuals from the current population for the next generation, thereby ensuring fitness levels are maintained[28].

(2) Crossover operator

The crossover operator is one of the key operations in GAs. It aims to generate new offspring individuals by combining chromosomes of parent individuals, thereby increasing genetic diversity and promoting population evolution. Common crossover methods include single-point crossover, multi-point crossover, and uniform crossover. In this paper, single-point crossover is adopted. According to the set crossover probability, a crossover point is selected in the individual genes. The gene segments before and after the crossover point are exchanged to generate two new individuals.

(3) Mutation operator

The mutation operator enhances population diversity by introducing random changes to individuals, preventing the algorithm from falling into local optimal solutions. Common mutation methods include basic bit mutation, uniform mutation, and non-uniform mutation. In this paper, basic bit mutation suitable for binary encoding is adopted. During this process, one or more bits on the chromosome are randomly selected and flipped (Changing 0 to 1 and 1 to 0) to introduce mutations.

(4) Adaptive mechanism

In traditional GAs, fixed crossover and mutation probabilities may cause the algorithm to fall into local optimal solutions. To address this issue, this paper adopts adaptive crossover probability P_c and mutation probability P_m to dynamically adjust the intensity of genetic operations. This avoids premature convergence of the algorithm, ensures its good exploration ability, and effectively improves the convergence speed and global optimization capability[32]. Crossover probability P_c and mutation probability P_m can be calculated by Eq.(9) and Eq.(10), respectively.

$$P_c=\begin{cases}P_{cmax}-\dfrac{(P_{cmax}-P_{cmin})(f-f_{avg})}{f_{max}-f_{avg}} & f\geqslant f_{avg}\\ P_{cmax} & f<f_{avg}\end{cases} \tag{9}$$

$$P_m=\begin{cases}P_{mmax}-\dfrac{(P_{mmax}-P_{mmin})(f_{max}-f')}{f_{max}-f_{avg}} & f'\geqslant f_{avg}\\ P_{mmax} & f'<f_{avg}\end{cases} \tag{10}$$

where P_{cmax} and P_{cmin} are the maximum and minimum crossover probabilities, respectively; f is the larger fitness value of the two individuals to be crossed; f_{avg} the average fitness value of the population; f_{max} the maximum fitness value of the population; P_{mmax} and P_{mmin} are the maximum and minimum mutation probabilities, respectively; and f' is the fitness value of the individual to be mutated.

As can be seen from the above equation, $f_{max}-f_{avg}$ is the value of the degree of convergence of the algorithm. When the algorithm converges to the local optimal value, the value of $f_{max}-f_{avg}$ will become smaller, and P_c and P_m should be increased to make the algorithm get rid of the local optimal value as soon as possible. $f-f_{avg}$ or $f_{max}-f'$ is used to value the excellence of the individual.

If the fitness value is lower than the average fitness value, the values of P_c and P_m increase with growing value of $f-f_{avg}$ or $f_{max}-f'$, indicating the quality of individual degraded. In this paper, $P_{cmax}=0.9$, $P_{cmin}=0.6$, $P_{mmax}=0.1$, $P_{mmin}=0.01$.

3.4 Construction of fitness functions

In GAs, the fitness function is a key indicator for the quality of individuals. The construction of fitness function directly affects the search direction and evolutionary results of GA, which can influence the solving effect of optimization problems. Typically, individuals with higher fitness are more likely to be retained and transmitted in genetic operations, such as selection, crossover, and mutation, thus improving the overall fitness level of the next generation.

For optimization problems, a common approach is to convert the objective function into a fitness function, ensuring that monotonically increasing relationship between fitness values and the quality of individuals can be established. In the optimization problem addressed in this paper, the objective function is transformed into the fitness function combined with the constraint condition.

When $D(X)$ is larger than 1, damage occurs inside the composite material. Even if the corresponding fitness value of the individual is high, the individual still fails to satisfy the constraints of the optimization problem and should therefore be discarded. When $D(X)$ is less than 1, no damage occurs inside the composite material. In this case, the higher the qualification rate of the individual's shape deviation, the larger the fitness value, indicating a better optimization effect of the individual.

To satisfy the requirements of both the constraint conditions and the objective function simultaneously, the objective function is converted as

$$F(X)=\begin{cases} R(X) & D(X)<1 \\ 0 & D(X)\geqslant 1 \end{cases} \tag{11}$$

where $F(X)$ represents the fitness function in the optimization problem addressed in this paper. A larger fitness function value indicates better fitness of the individual and a more optimal corresponding optimization scheme. This helps GA to preferentially select and retain individuals with high fitness during the evolution process, thereby gradually screening out the optimal solution.

3.5 Set termination conditions

In the application of GAs, common termination conditions include selecting the optimal solution after a fixed number of iterations, selecting the optimal solution after a fixed running time, or stopping the calculation when a preset optimization target is achieved. In this paper, the termination condition is set as selecting the optimal solution after a fixed number of iterations. By setting different numbers of iterations, when the optimal solution value of GA tends to be stable, the optimization model can be considered to have obtained an ideal solution.

4 Initialization of Finite Element Model

To calculate the stress and predict the damage initiation in the composite panel during the shape optimization, an initial finite element model of the composite panel based on the actual shape should be created. The whole process includes generation of the actual model for the panel, set material properties, definition of mesh, and determination of monitoring points and other operations.

4.1 Generation of the model for the composite panel

A critical step in the generation of the finite element model for composite materials is to obtain the actual profile of the panel. In this paper, high-precision 3D laser scanning technology is adopted to collect the point cloud data of the panel surface. Based on the Geomagic Wrap software, preprocessing operations, such as denoising, simplification, and smoothing, are performed on the original point cloud data to ensure that the data quality meets the modeling requirements. Then, reverse engineering modeling is conducted to reconstruct a high-fidelity solid model of the composite panel based on the processed point cloud data. Finally, an accurate geometric basis is provided for subsequent finite element analysis.

4.2 Element type selection and meshing

To ensure the accuracy of the analysis results,

an eight-node linear hexahedral reduced-integration element (C3D8R) is chosen for the mesh of the composite panel in this paper. This element type can achieve high calculation accuracy and good convergence. Moreover, the phenomenon of shear self-locking can be avoided effectively. Thus C3D8R is suitable for the stress-strain analysis of composite structures involved in this paper.

4.3 Material property settings

Common modeling methods for composite panels include conventional shell layup, continuum shell layup, and solid layup. To accurately simulate the stress state of the panel, the solid element layup method is used and the material properties of the composite panel are defined based on the actual condition in this paper.

As mentioned before, 3D Hashin criterion is employed in this paper to assess whether damage has occurred in composite materials. To accurately characterize the damage evolution behavior of composite material structures, six user-defined variables (User output variables) have been introduced in the material property definition, corresponding to the initiation and development criteria of six damage modes in composite materials. A specialized UVARM subroutine has been developed through the Fortran interface of ABAQUS software and integrated into the ABAQUS/Standard solver, achieving secondary development at the solver level.

4.4 Monitoring point setting

Quantitative analysis of the profile compliance of panels is conducted via PolyWorks software. The theoretical model and the measured point cloud data are imported into the software. Once the coordinate system registration is completed, the deviation nephogram can be generated to show the overall distribution of deviations. Considering the requirements for a quantitative description of profile compliance, the arrangement of monitoring points (nodes) is determined based on the meshing of the subsequent finite element model.

In the process of finite element modeling, a displacement monitoring point is set every n elements to establish an equidistant displacement monitoring network. After setting up the monitoring points, the initial shape deviation of the panel is obtained by entering the coordinates of the monitoring points in the PolyWorks software. In the process of solving the optimization scheme, the displacement change of the monitoring point is obtained by running a Python script in ABAQUS, and the fitness function after applying the load is calculated to determine the profile compliance of the panel after shape control.

5 Validation of Shape Optimization Strategy

As shown in Fig.5, the assembly process of the wing-body fairing panel is selected to validate the shape optimization strategy proposed in this paper. First, the position of the panel is accurately determined via the positioning module on the tooling. Second, the initial point cloud data of the panel is obtained through digital measurement methods, and the actual model of the panel is constructed using reverse modeling technology. Based on the shape optimization strategy proposed in this paper, the layout distributed shape-adjusting ends and displacement magnitude of every distributed shape-adjusting end are obtained. Finally, the optimal layout of distributed shape-adjusting ends and displacement of each end are used to meet the requirements on the profile compliance of the composite panel.

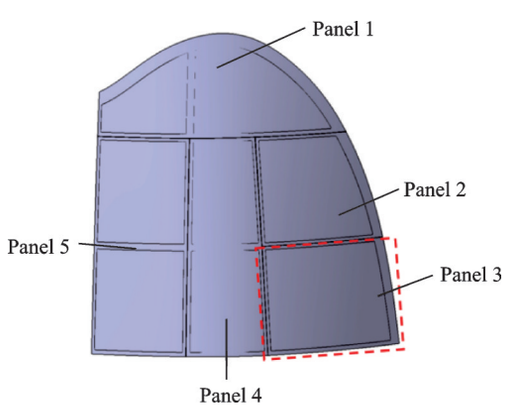

Fig.5 Test piece of wing-body fairing of an aircraft

5.1 Subjects

Owing to the size of flexible tooling, Panel 3, shown in Fig.5, is selected to conduct further study. The maximum length of Panel 3 is approximately 2 070 mm, the width is approximately 1 274 mm, and the thickness is approximately 8 mm.

The flexible tooling, involved in this paper, consists of tooling frame, positioning modules, distributed shape-adjusting ends, control system, and other accessories. The positioning module consists of adjustable positioning blocks, which enables precise positioning of the panel through positioning holes. Corresponding assembly holes have been prepared on the panel. Once the panel is placed on the tooling, its spatial position is fixed by multiple positioning modules on the tooling and constraints are used. Then, marker points are fixed on the surface of the panel test piece for subsequent measurements based on a 3D scanner. The positioned Panel 3 is shown in Fig.6.

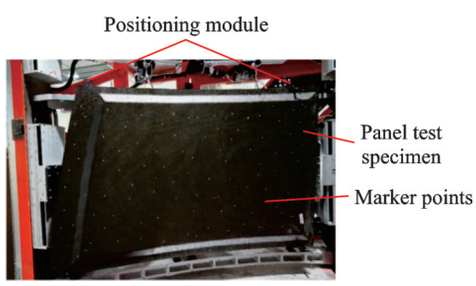

Fig.6 Composite panel test specimen

The shape-adjusting ends consists of vacuum suction cups, servo motors, guide rails, and other accessories. The displacement can be adopted in the normal direction of the panel surface. The vacuum suction cups are controlled to move along the three directions by a servo motor. It is also equipped with pressure sensors and displacement sensors to monitor the force and the displacement used during the shape optimization of the composite panel. The radius of the vacuum suction cup is 40 mm, where a vacuum degree of −60 kPa can be generated. Thus, the adsorption force of the vacuum suction cup is too small to introduce the local deformation of the composite panel. So the effect of suction cup adsorption is ignored. The structure of the shape-adjusting ends and its distribution on the surface of the panel are shown in Fig.7.

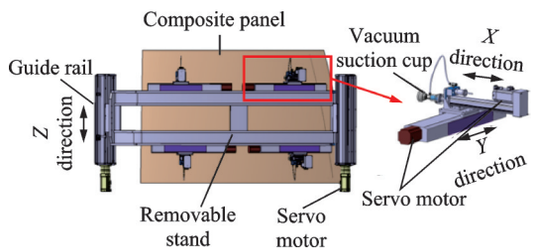

Fig.7 Schematic diagram of the shape-adjusting ends

5.2 Reverse modeling and deviation analysis

In consideration of the openness of the tooling, the measured point cloud data of the panel's outer surface is obtained by KSCAN-Magic Ⅱ three-dimensional laser scanner. Combined with Geomagic Design X software, a model of the actual panel's outer surface can be generated. The error between the reversed model surface and measured point cloud date is obtained via automatic calculation based on the volume deviation function in Geomagic Design X software.

As shown in Fig.8, the error between the outer surface of reversed model and the original point cloud data is mostly less than 0.05 mm, which means that high-fidelity reconstruction has been conducted. As the thickness of Panel 3 is 8 mm, a solid model of Panel 3 can be developed based on the outer surface of reversed model for subsequent finite element analysis.

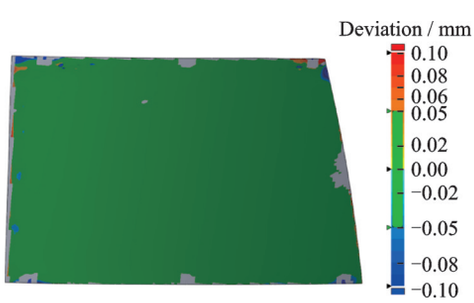

Fig.8 Accuracy analysis of panel obtained by reverse modeling

The shape deviation between the actual profile and theoretical profile of the composite panel can be obtained by deviation analysis function of PolyWorks software in the same coordinate system. To

balance computational accuracy and computational efficiency, the mesh size is set to 20 mm in the finite element model. A displacement monitoring point is set every 2 meshes via a Python script. A total of 1 306 monitoring points can be generated on the surface of Panel 3, in which the interval between monitoring points is approximately 40 mm. Once the coordinates of the monitoring points are imported into PolyWorks, initial deviation values of all monitoring points are obtained, which serve as the calculation basis for the rate of profile compliance in subsequent shape optimization. The initial shape deviation is shown in Fig.9.

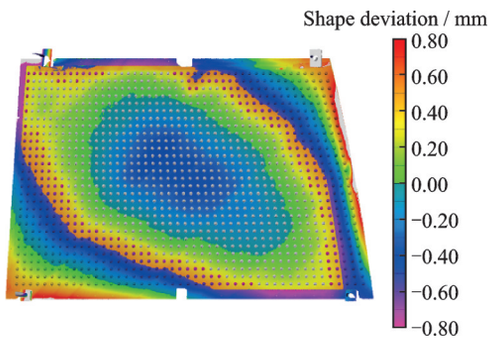

Fig.9 Initial shape deviation distribution diagram

5.3 Establishment of finite element model

As mentioned in Section 4, a finite element model of a composite panel should be established for stress analysis and the prediction of damage. To obtain good accuracy of numerical results, the material parameters are assigned to the composite panel, which is provided by the manufacture of composite materials. The thickness of each ply is 0.2 mm and the layup sequence is $[0/90]_{20}$. More details can be seen in Table 1.

Table 1 Material parameters of plain weave single laminate

Property	Value	Property	Value
E_{11}/GPa	21	X_t/MPa	322
E_{22}/GPa	23	X_c/MPa	364
E_{33}/GPa	18	Y_t/MPa	322
ν_{12}	0.20	Y_c/MPa	364
ν_{13}	0.15	Z_t/MPa	103
ν_{23}	0.15	Z_c/MPa	500
G_{11}/GPa	2.65	S_{12}/MPa	118
G_{13}/GPa	1.7	S_{13}/MPa	24
G_{23}/GPa	1.7	S_{23}/MPa	24

To improve computational efficiency, the spatial layout of the distributed shape-adjusting ends is considered as a set of representative positions during the finite element analysis. As the motion stroke of shape-adjusting ends in Y and Z directions is 200 mm, three positions can be chosen where the distance between each point is 100 mm. Thus, the typical layout configuration of a single suction cup includes nine different displacement application points, as shown in Fig.10. This simplification not only ensures the accuracy of mechanical analysis, but also significantly reduces the complexity of solving contact nonlinear problems.

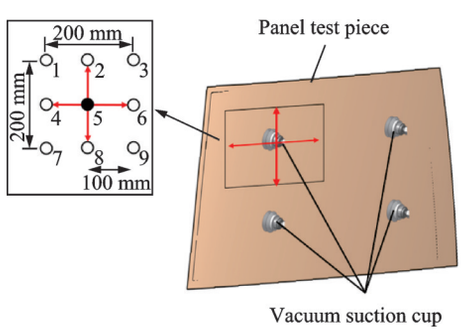

Fig.10 Typical layout for vacuum suction cup

As shown in Fig.10, four distributed shape-adjusting ends are equipped in the tooling for the shape optimization of the composite panel. Each vacuum chuck has nine displacement application points, resulting in a total of 36 displacement application points. These points correspond to 36 mesh nodes in the finite element model, which are numbered as RP-i-k ($i \in [1,2,3,4]$, $k \in [1,2,\cdots,9]$). The interaction between the suction cup and the composite panel is simplified as a coupling constraint between the displacement application points and the mesh node on the panel surface. A continuously distributed coupling is adopted, which are numbered as Constraint-i-k ($i \in [1,2,3,4]$, $k \in [1,2,\cdots,9]$). The influence radius of the coupling constraint is consistent with the radius of the suction cup, as shown in Fig.11.

Since the composite panel is a curved panel, the displacement applied by the vacuum suction cup is the normal direction of the curve panel at the dis-

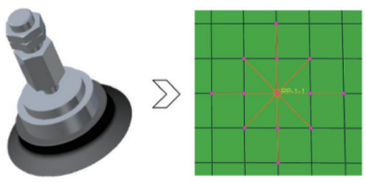

Fig.11 Schematic diagram of the coupling constraint of the vacuum suction cup

placement application points. Thus, a local cylindrical coordinate system is established at the displacement application points of each vacuum suction cup, numbered as Datum csys-i-k ($i \in [1,2,3,4]$, $k \in [1,2,\cdots,9]$).

In the actual shape optimization process, the displacement applied on the panel is controlled by movement of the vacuum suction cups along the Z direction in its local coordinate system, which are numbered as Displacement-i-k ($i \in [1,2,3,4]$, $k \in [1,2,\cdots,9]$).

Based on the positioning method of the composite panel on the tooling, corresponding boundary conditions are set, where fully fixed constraints are used at the corresponding positions of the panel (U1 = U2 = U3 = UR1 = UR2 = UR3 = 0). The finite element model is shown in Fig.12.

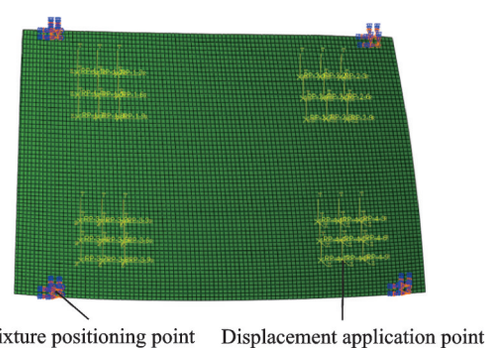

Fig.12 Finite element model of composite panel

5.4 Solution for shape control scheme of the panel

Based on the finite element model established in Section 5.3, the optimization objective of this study is to find out no more than four points from the 36 displacement application points and get appropriate displacement loads to reduce the deviation between the actual and theoretical profiles of the panel under the premise that no damage is initiated in the composite panel. The domain for the design variables can be defined as $n \leqslant 4$. According to the actual parameters of vacuum suction cup, L_{max} is set as 3 mm.

According to the assembly process specifications of the wing-body fairing panel, the allowable value of the shape deviation of the panel is $\Delta\omega = 0.3$ mm. Then, the shape optimization scheme can be achieved through an iterative combination of GAs and the proposed finite element calculations. Parameters of GA are shown in Table 2.

Table 2 Parameters of GA

Parameter	Value
Initial population size	10
Population size maintained during iteration	12
Maximum crossover probability	0.9
Minimum crossover probability	0.05
Maximum mutation probability	0.5
Minimum mutation probability	0.05
New individuals created by mutation	5
New individuals randomly generated	5
Good individuals retained to the next generation	2
Good individuals output to file in each iteration	10

The optimization scheme is performed on a standard desktop computer with an Intel Core i7 processor and 16 GB of RAM. After 55 iterations. It takes 2 h and 23 min to eliminate repeated shaping, showing high computational efficiency of the proposed optimal method.

The termination condition of the GA is defined as the optimal solution after a fixed number of iterations. The maximum evolutionary algebra T is set to 5, 15, 25, 35, 45, and 55 generations. The maximum fitness values of the current population with different number of iterations are shown in Fig.13.

As illustrated in Fig.13, when T=55, the fitness value of the optimal solution does not improve further. Same fitness value can be obtained in 15 consecutive generations. Therefore, the optimization result is obtained with the termination condition of T=55, and the maximum fitness in the final population is the optimal solution for the shape optimiza-

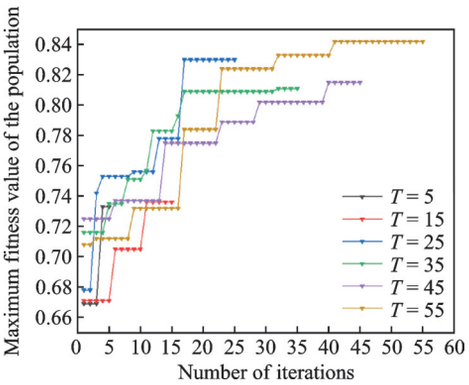

Fig.13 Iterative results of GA

tion of the composite panel. In such condition, the optimal layout of distributed shape-adjusting ends is $H=\{4, 5, 6, 4\}$, the optimal displacement of distributed shape-adjusting ends is $L=\{2.27, 1.97, 2.28, 1.70\}$, and the profile compliance rate is $R(X)=0.842$. The optimal layout of distributed shape-adjusting ends in ABAQUS is shown in Fig.14.

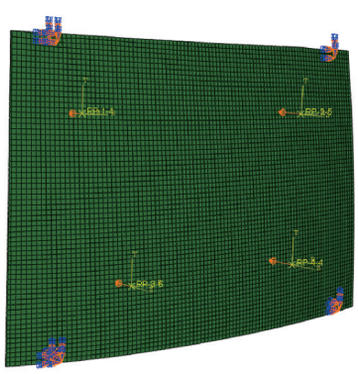

Fig.14 Optimal vacuum cup positions identified by GA

5.5 Shape optimization and result analysis

Based on the optimal strategy of the panel obtained in Section 5.4, the distributed shape adjustment ends are moved to corresponding position and the right displacement are used, as shown in Fig.15. Meanwhile, the force sensor can record the force applied on the panel during the shape optimization.

Surface of the panel after optimization can be obtained via the KSCAN-Magic Ⅱ 3D scanner. Then the deviation nephogram between the optimal shape and the theoretical shape can be seen in Fig.16. Compared with Fig.9, the deviation between actual and theoretical shapes after optimization is more uniform than that before optimization.

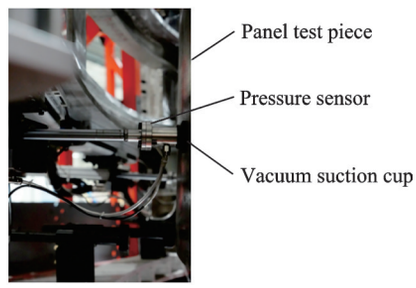

Fig.15 Applying displacement during shape control

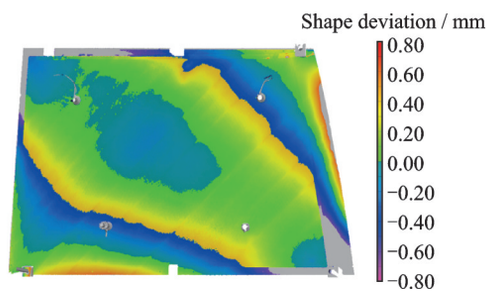

Fig.16 Shape deviation nephogram between measured and theoretical data after shaping

As shown in Fig.17, a comparative analysis of the shape adjustment effect of the composite panel is conducted via histogram statistical analysis. The horizontal axis represents the deviation range, and the vertical axis indicates the frequency distribution of monitoring points in each deviation range. Experimental data indicate that the number of monitoring points, whose deviation is less than 0.2 mm, increases significantly after shape optimization compared with that before optimization. The average shape deviation before and after optimization is 0.236 and 0.147 mm, respectively. Statistical analysis of the deviation value information of the monitoring points, a total of 1 119 displacement monitoring points (out of 1306), are within the deviation range of 0.3 mm. The rate of profile compliance (deviation is less than 0.3 mm) increases from 66.46% before adjustment to 86.36% after adjustment, with an improvement of 19.9%.

As the rate of profile compliance obtained via the finite element analysis is 84.2%, the deviation between the experimental and the numerical results is only 2.16%. Thus, the accuracy of the optimization strategy proposed in this paper is verified.

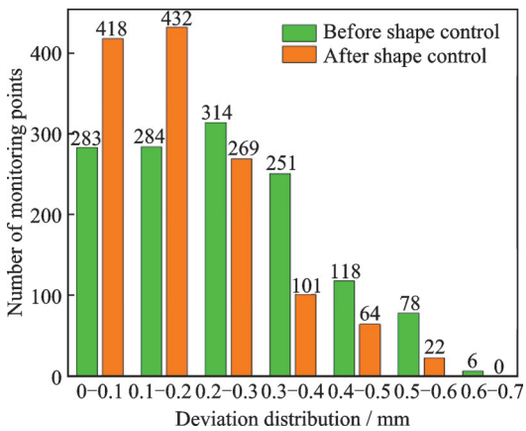

Fig.17 Histogram of the deviation value of monitoring points before and after adjustment

To further verify the effectiveness and necessity of the shape control scheme for the panel proposed in this paper, a comparative experiment is set up: The panel without shape control is used as the control group. Using the framework as the assembly reference, the panel is directly fitted to the framework, applying positioning constraints to the panel by inserting temporary fasteners through the assembly of the initial holes. After the constraints are completed, the KSCAN-Magic Ⅱ 3D laser scanner is used to measure the contour surface of the panel. The measured point cloud data is then compared and analyzed with the theoretical shape of the panel in PolyWorks software, and the coordinates of the displacement monitoring points are also imported. The shape deviation nephogram is shown in Fig.18. Statistical analysis of the deviation values for each monitoring point shows that 845 monitoring points fall within the deviation range of 0.3 mm, resulting in a calculated qualified rate of shape deviation of 63.34%.

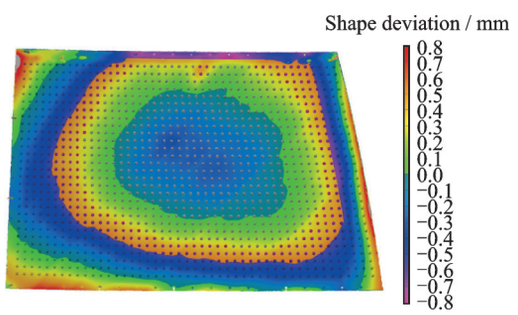

Fig.18 Shape deviation nephogram of the control group

The above data demonstrate that compared to the conventional rigid tooling (63.34% qualified rate) and existing shape control methods, the proposed strategy achieves three key advantages: Higher accuracy (85.68% qualified rate), superior uniformity (reduction of outliers above 0.3 mm), and enhanced efficiency (2 h 2 min optimization time). This validates its competitiveness for high-precision composite assembly.

6 Conclusions

(1) To address the issue of shape control for composite panels, an optimal shape control method for composite panels is proposed by combining FEA with an adaptive GA in this study. Taking the minimum deviation between the actual shape and theoretical shape of the composite panel as the objective, and taking no introduction of defects into the composite material as the constraint, this method automatically obtains the optimal layout of shape adjustment units and the displacement magnitude applied by each shape adjustment unit.

(2) In this study, the traditional GA is improved. Genetic operator operations including roulette selection, single-point crossover and basic bit mutation are adopted. The convergence and global search capability of the algorithm are optimized by integrating an adaptive mechanism, enabling efficient optimization of design variables. The feasibility of the optimization scheme is verified through finite element simulation.

(3) The proposed profile optimization method is verified through a case study on the panel of a aircraft wing-body fairing based on the flexible tooling. The results show that the optimization scheme increases the accuracy of shape matching from 66.46% to 86.36%, with an improvement of approximately 20%, and the deviation distribution is more uniform. This method can provide valuable engineering references for the collaborative control of shape and performance of aviation composite structures.

Although the proposed optimization strategy

has achieved good results under ideal conditions, the possible influence of the tooling itself on the panel has not been considered in practical application. For example, the adsorption effectiveness of vacuum suction cups can be affected by surface conditions and small leaks, while sensor noise can also lead to inaccurate measurement data. To address these challenges, mitigation strategies including surface preparation of composites, vacuum cup seal integrity checks, and sensor noise filtering should be employed. These improvements not only help to improve the accuracy of the shape control of composite panels but also enhance the adaptability and stability of the technology in practice.

References

[1] DU Shanyi. Advanced composite materials and aerospace engineering[J]. Acta Materiae Compositae Sinica, 2007, 24(1): 1-12. (in Chinese)

[2] NING Li, YANG Shaochang, LENG Yue, et al. Overview of the application of advanced composite materials on aircraft and the development of its manufacturing technology[J]. Composites Science and Engineering, 2020(5): 123-128. (in Chinese)

[3] MA Limin, ZHANG Jiazhen, YUE Guangquan, et al. Application of composites in new generation of large civil aircraft[J]. Acta Materiae Compositae Sinica, 2015, 32(2): 317-322. (in Chinese)

[4] ARISTA R, FALGARONE H. Flexible best fit assembly of large aircraft components. airbus A350 XWB case study[C]//Proceedings of Product Lifecycle Management and the Industry of the Future. Cham: Springer, 2017: 152-161.

[5] LI Dongsheng, YANG Yingke, ZHAI Yunong, et al. Research on shape and force control technology for commercial aircraft CFRP fuselage panel assembly[J]. Acta Materiae Compositae Sinica, 2022, 39(9): 4310-4318. (in Chinese)

[6] SÖDERBERG R, WÄRMEFJORD K, LINDKVIST L. Variation simulation of stress during assembly of composite parts[J]. CIRP Annals, 2015, 64(1): 17-20.

[7] LIU Zhenyang, ZHAI Yunong, LI Dongsheng, et al. Research and application progress of deformation control technology for aircraft composite panel assembly[J]. Aeronautical Manufacturing Technology, 2022, 65(18): 46-54, 78. (in Chinese)

[8] LUO Qun, WANG Qing, LIU Zhizheng, et al. Wing-fuselage compliant docking assembly and contact force analysis method[J]. Journal of Nanjing University of Aeronautics & Astronautics, 2022, 54(3): 439-449. (in Chinese)

[9] RAMIREZ J, WOLLNACK J. Flexible automated assembly systems for large CFRP-structures[J]. Procedia Technology, 2014, 15: 447-455.

[10] YANG Yingke, LI Dongsheng, SHEN Liheng, et al. Pose and shape adjustment method for CFRP fuselage panel based on multi-robot collaboration[J]. Acta Aeronautica et Astronautica Sinica, 2023, 44(14): 428006. (in Chinese)

[11] LIU C Q, HONG J, WANG S F. Multi-point positioning method for flexible tooling system in aircraft manufacturing[C]//Proceedings of the ASME 2012 International Mechanical Engineering Congress and Exposition. Houston, USA: American Society of Mechanical Engineers, 2012,3: 113-117.

[12] LIU Chunqing, HONG Jun, FENG Yan, et al. Searching optimization algorithm for deformation control of aircraft thin-walled parts in multi-point flexible tooling system[J]. Journal of Shanghai Jiao Tong University, 2013, 47(8): 1191-1197. (in Chinese)

[13] WU F F, LI D S, DU B R. Optimal assembly of a skin panel onto the fuselage framework based on force control technology[J]. Proceedings of the Institution of Mechanical Engineers, Part E: Journal of Process Mechanical Engineering, 2016, 230(6): 447-451.

[14] ZHANG Qiuyue. Optimization of size and layout of pressing force for composite airframe structure assembly[D]. Nanjing: Nanjing University of Aeronautics and Astronautics, 2019. (in Chinese)

[15] ZHANG Qiuyue, AN Luling, YUE Xuande, et al. Optimization of size and layout of pressing force for composite airframe structure assembly based on genetic algorithm[J]. Acta Materiae Compositae Sinica, 2019, 36(6): 1546-1557. (in Chinese)

[16] ZHANG W, AN L L, CHEN Y, et al. Optimisation for clamping force of aircraft composite structure assembly considering form defects and part deformations[J]. Advances in Mechanical Engineering, 2021, 13(4): 1687814021995703.

[17] JIANG Ce. A shape control technology of aircraft CFRP panel based on flexible assembly tooling[D]. Nanjing: Nanjing University of Aeronautics and Astronautics, 2022. (in Chinese)

[18] ZHANG Dewei. A shape control technology of aircraft composite radome hood[D]. Nanjing: Nanjing University of Aeronautics and Astronautics, 2024. (in Chi-

nese)

[19] YANG D, QU W W, KE Y L. Evaluation of residual clearance after pre-joining and pre-joining scheme optimization in aircraft panel assembly[J]. Assembly Automation, 2016, 36(4): 376-387.

[20] YU Xiaonan, XU Xiwu, GUO Shuxiang, et al. Performance research of asymmetric variable thickness composite laminate under compressive load[J]. Journal of Nanjing University of Aeronautics & Astronautics, 2024, 56(1): 103-115. (in Chinese)

[21] SI Suo, WANG Hua. Simulation and modeling research on effect of R-angle deviation of C-section composites beam on static load strength in assembly[J]. Aeronautical Manufacturing Technology, 2016, 59(10): 93-97. (in Chinese)

[22] YANG B F, YUE Z F, GENG X L, et al. Experimental and numerical study on bearing failure of countersunk composite-composite and composite-steel joints[J]. Journal of Composite Materials, 2017, 51(22): 3211-3224.

[23] YE J X, YAN Y, LI J, et al. 3D explicit finite element analysis of tensile failure behavior in adhesive-bonded composite single-lap joints[J]. Composite Structures, 2018, 201: 261-275.

[24] LI Xueting, AN Luling, YUE Xuande, et al. Optimization method of the number and layout of temporary fasteners in composite panel assembly of aircraft[J]. Acta Materiae Compositae Sinica, 2022, 39(8): 4102-4116. (in Chinese)

[25] FENG Hao, ZHOU Yadong, DING Cong, et al. Aircraft noise prediction based on machine learning model[J]. Transactions of Nanjing University of Aeronautics and Astronautics, 2023, 40(S2): 54-61.

[26] ZHOU Yi, HU Minghua, YANG Lei, et al. Collaborative conflict-free 4D trajectory planning based on multi-objective hybrid-metaheuristic optimization algorithm[J]. Transactions of Nanjing University of Aeronautics and Astronautics, 2024, 41(3): 372-386.

[27] MA Yongjie, YUN Wenxia. Research progress of genetic algorithm[J]. Application Research of Computers, 2012, 29(4): 1201-1206, 1210. (in Chinese)

[28] BIAN Xia, MI Liang. Development on genetic algorithm theory and its applications[J]. Application Research of Computers, 2010, 27(7): 2425-2429, 2434. (in Chinese)

[29] LIU Yang, HUANG Yong, WU Yuzhu, et al. Layout optimization design and system development of machining workshop based on genetic algorithm[J]. Mechanical Engineer, 2024(5): 13-17. (in Chinese)

[30] JIANG Renjie, YANG Xiaoguang, SHI Duoqi, et al. Complex structure life calculation platform based on secondary development of Abaqus[J]. Journal of Mechanical Strength, 2024, 46(1): 216-223. (in Chinese)

[31] ZHANG Chaoqun, ZHENG Jianguo, QIAN Jie. Comparison of coding schemes for genetic algorithms[J]. Application Research of Computers, 2011, 28(3): 819-822. (in Chinese)

[32] YAN Weimiao. Study on technologies for controlling and correcting large aircraft panel assembly deformation[D]. Hangzhou: Zhejiang University, 2015. (in Chinese)

Acknowledgement This work was supported by the Research Startup Project of Nanjing University of Aeronautics and Astronautics (No.90YAH24038).

Authors

The first author Mr. **WANG Qi** is currently an engineer of AVIC Research Institute for Special Structures of Aeronautical Composites. His research focuses on the aircraft assembly technology.

The corresponding author Dr. **ZHAO Cong** received the Ph.D. degree in material manufacture engineering at Nanjing University of Aeronautics and Astronautics in 2017. Currently, he is an associate professor in College of Mechanical and Electrical Engineering, Nanjing University of Aeronautics and Astronautics. His research has focused on the advanced manufacturing technology of composite part, assembly technology of aircraft, etc.

Author contributions Mr. **WANG Qi** designed the study, complied the models, conducted the analysis, interpreted the results and wrote the manuscript. Mr. **ZHANG Pin** designed the study and supported the analysis. Mr. **YU Jixuan**, and Mr. **MENG Xiangmin** contributed to data and material for validation experiment. Mr. **WANG Kuikui** contributed to the discussion and background of the study. Dr. **ZHAO Cong** contributed to algorithm development, supported the analysis, and revised the manuscript. Mr. **ZHANG Xuezhuang** and Ms. **LI Xinxin** contributed to the manuscript and establishment of optimization model. All authors commented on the manuscript draft and approved the submission.

Competing interests The authors declare no competing interests.

(Production Editor: XU Chengting)

基于柔性工装的飞机复材壁板外形调控优化策略

王 琦[1]，张 聘[1]，于吉选[1]，孟祥敏[1]，王魁奎[1]，赵 聪[2]，张学壮[2]，李欣欣[2]

（1.中国航空工业集团公司济南特种结构研究所高性能电磁窗航空科技重点实验室，济南 250023，中国；
2.南京航空航天大学机电学院，南京 210016，中国）

摘要：碳纤维复合材料凭借高比强度、高比模量以及优异的轻量化特性，现已广泛应用于现代航空飞行器主承力与大型气动外形结构。在热压成形工艺下，复合材料构件易因树脂固化收缩、热应力耦合作用以及铺层结构约束差异产生不可避免的固化变形，致使构件理论设计型面与实际成形型面之间存在明显偏差。该外形偏差会直接劣化飞机气动外形精度，降低结构装配协调性，严重制约大型复合材料构件在航空装备中的高精度装配应用。因此，开展复合材料构件装配外形主动调控技术研究，对消除固化变形误差、保障飞行器气动外形准确度、提升整机装配质量具有重要工程意义。针对大尺寸飞机复合材料壁板装配过程中普遍存在的外形偏差校正困难、调形位移难以定量求解、调控过程易诱发材料内部损伤等工程难题，本文提出一种融合有限元仿真与自适应遗传算法的协同优化调形方法。以复合材料结构损伤约束为边界条件，在严格保证构件内部不产生分层、基体开裂等力学损伤的前提下，对各调形执行末端的位移量进行智能迭代求解，实现复合材料壁板实测外形与理论设计外形之间的偏差最小化。为验证所提优化策略的工程可行性与有效性，本文以某型机翼身整流罩复合材料壁板为研究对象，建立对应的数值仿真模型并开展外形调形优化分析。研究结果表明：采用本文协同优化方法后，复合材料壁板外形偏差消除率由初始66.46%提升至86.36%，构件外形偏差分布均匀性得到显著改善；同时，全过程结构应力均处于材料许用范围，实现了无损伤精准调形。本方法有效解决了传统被动校正方式精度低、一致性差、易产生二次损伤的技术短板，可为航空复合材料大型构件数字化、高精度装配调形提供可靠的技术参考，同时为同类飞行器薄壁复合材料结构的外形精准控制提供新的优化思路与工程应用途径。

关键词：复合材料；飞机装配；外形调控；优化策略；遗传算法

研究亮点：

1.针对大尺寸复合材料壁板固化变形导致的装配偏差难题，构建有限元仿真与自适应遗传算法相结合的协同优化调形方法，突破传统被动校正手段精度低、随机性强的局限，实现调形位移的智能定量求解。

2.所提优化方法可有效提升复合材料构件装配精度与偏差均匀性，且该方法具备良好的适应性，为航空复合材料构件数字化精密调形提供可靠技术方案。